ELSEVIER

Journal of Nuclear Materials 253 (1998) 10–19

journal of nuclear materials

Computation of the lamina stacking sequence effect on elastic moduli of a plain-weave Nicalon/SiC laminated composite with a [0/30/60] lay-up

Wei Zhao [a,*], Peter K. Liaw [b], Niann-i Yu [c]

[a] *Department of Material Sciences and Engineering, 323 Dougherty Engineering Building, University of Tennessee, Knoxville, TN 37996-2200, USA*

[b] *Department of Material Sciences and Engineering, 427B Dougherty Engineering Building, University of Tennessee, 427-B Dougherty, Knoxville, TN 37996-2200, USA*

[c] *Department of Mechanical and Aerospace Engineering and Engineering Science, University of Tennessee, 414 Dougherty, Knoxville, TN 37996-2210, USA*

Abstract

Estimation of the elastic modulus is important in engineering design. One difference between CFCCs (continuous fiber-reinforced ceramic–matrix composites), and CMCs (whisker, particulate, or short fiber-reinforced ceramic–matrix composites), is that the anisotropic behavior of CFCCs plays an important role in affecting their mechanical behavior. This feature may also contribute to the variation of elastic properties and strengths of CFCC. In this paper, a Fortran program is developed to quantify the lamina stacking sequence effect on the effective elastic moduli of the laminated CFCCs. The material for modeling is a plain-weave Nicalon fiber-reinforced silicon carbide (Nicalon/SiC) CFCCs. Results show that various stacking sequences within the CFCC (a [0/30/60] lay-up) will give different effective elastic moduli of the CFCCs. This trend leads to a variation of the slope of the linear portion on the flexural stress–strain curve, i.e., changing the position of the starting point of the non-linear portion, and the shape of the whole curve, which gives a different value of the peak stress in the curve.

1. Introduction

Continuous fiber-reinforced ceramic–matrix composites (CFCCs) have shown a great potential as high-temperature structural materials due to their non-catastrophic, 'graceful' failure behavior. Furthermore, CFCCs retain all other excellent properties of monolithic ceramics, such as light weight, good thermal conductivity, high specific strength, high specific stiffness, high resistance of corrosion, wear, and oxidation, etc. [1–3]. The pertinent applications of CFCCs include energy production facilities (e.g., heat exchangers, combustors, hot-gas filters, boiler components, first walls and high heat flux surfaces), and aerospace industry (e.g., structural and machinery components) [4–6].

One feature difference in microstructures between CFCCs and other types (whisker, particulate, short fiber-reinforced) of ceramic matrix composites (CMCs) is the strong anisotropic behavior of CFCCs. This implies that the effect of the in-plane fiber fabric orientation would contribute more significantly to the mechanical behavior of the laminated CFCCs than that of CMCs. It is likely that this factor may also lead to the scatter of elastic properties and flexural strength of CFCCs. Understanding this fabric orientation effect definitely will help to minimize the influence of this effect on mechanical performance, and will also provide a better understanding of the contributions of other dominant parameters, such as interfacial coating properties.

For the Nicalon fiber fabric-reinforced SiC (Nicalon/SiC) composite fabricated by the forced-flow thermal gradient chemical vapor infiltration (FCVI) method, some experimental work has been conducted to

* Corresponding author. Fax: +1-423 974 4115; e-mail: wzhao@nestor.engr.utk.edu.

0022-3115/98/$19.00
PII S0022-3115(97)00320-6

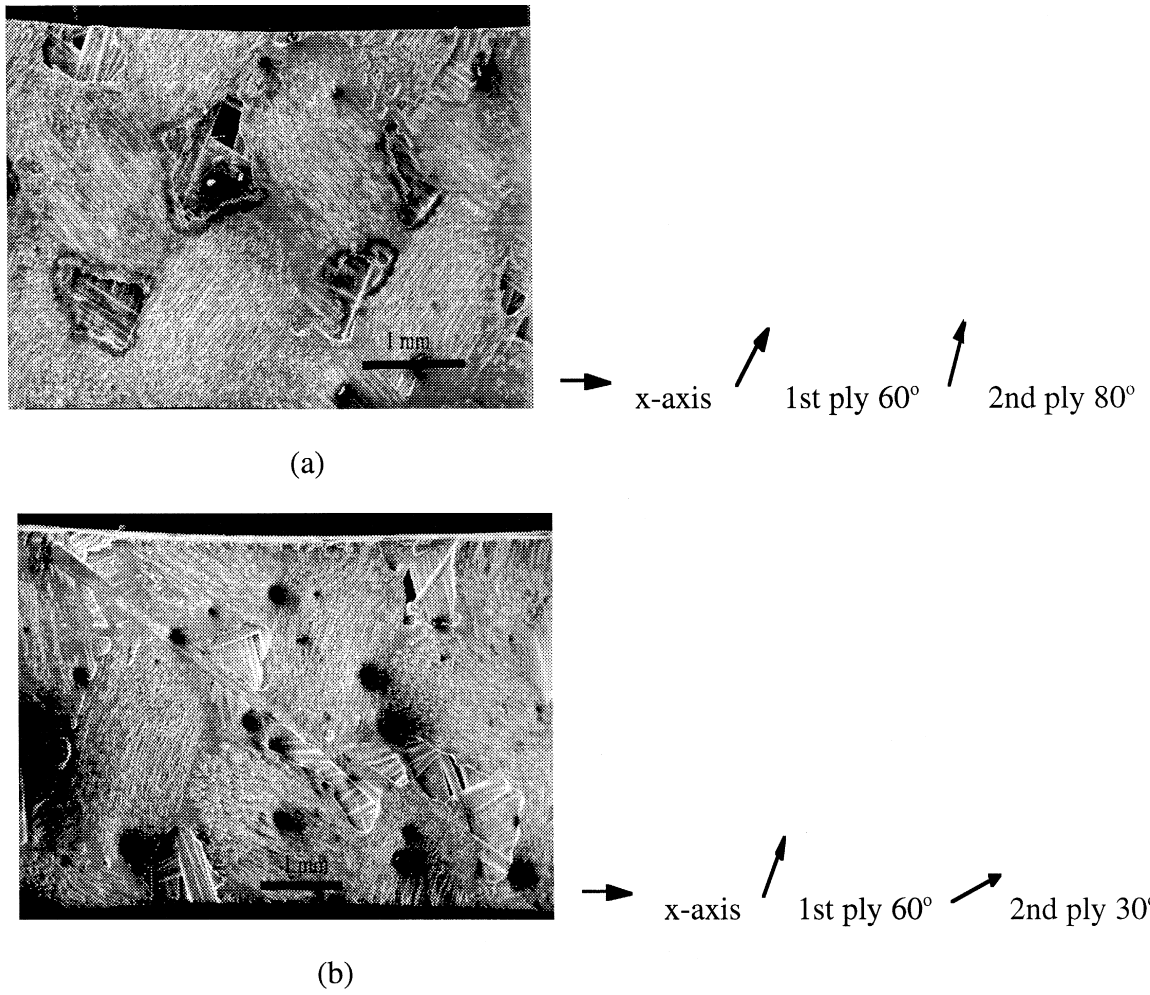

Fig. 1. Micrographs showing differences in stacking sequences of two laminates.

estimate the effective elastic moduli of the laminated CFCC. However, little attention has been paid to the effects of lamina lay-up, and the lamina stacking sequence within the same lay-up, on mechanical properties of CFCCs [4–8]. In this paper, the influence of the lamina stacking sequence within one [0/30/60] lay-up on laminate effective elastic moduli was investigated on a plain-weave, non-symmetrical Nicalon/FCVI-SiC CFCC. The computation model is established by developing a Fortran program, based on the classical laminated plate theory [9–13]. A fiber undulation model is also employed to compute the reduced stiffness matrix for the plain-weave geometry [14]. Fig. 1 shows the fiber fabric orientation from the tensile side of laminates and it is evident that the two laminates have different stacking sequences.

To facilitate the computation, it is better to clarify the terminology of lay-up, stacking series and the stacking sequence. Lay-up is the configuration of the laminate indicating its ply composition, such as: [0/30/60], [0/45], [−60/0/60], and [0/90], etc. Stacking series is the configuration indicating one possible combination of the ply arrangement within a certain lay-up, which can be repeated to form the whole sequence of the laminate. Within the [0/30/60] lay-up, there are six possible combinations of stacking series, i.e., [0/30/60], [30/60/0], [60/0/30], [60/30/0], [0/60/30], and [30/0/60]. Within the [0/45] lay-up, there are two combinations of stacking series, [0/45] and [45/0]. Stacking sequence is the configuration indicating the exact location and arranging order of the various plies, such as: $[0/30/60]_4$, $[0/45]_6$, $[0/30/60/0/30/\ 60/0/30]_T$, etc. (note that the subscript T stands for total).

2. The material system for modeling

The material chosen for modeling is a 40 volume percentage plain-weave Nicalon fiber fabric-reinforced

FCVI-SiC composite processed at the Oak Ridge National Laboratory (ORNL). The Nicalon fiber fabrics are commercial products of Nippon Carbon, which mainly contain Si, C and O with a weight ratio of 6:3:1. The fiber preform was cut into a disk shape with a diameter of 7.62 cm. Then, the disk-shaped preform was stacked by the [0/30/60] lay-up, with about 50 plies per 1.27 cm, i.e., the average thickness of one plain-weave lamina is 0.0254 cm. Firstly, the fiber preform was deposited with certain interfacial coatings, such as C and/or SiC, by a conventional chemical vapor deposition (CVD) method. The preform was then put into a cylindrical FCVI chamber to be infiltrated to obtain the SiC matrix through the decomposition of methyltrichlorosilane (MTS) in hydrogen at approximately 1000°C for about 24 h. The density of the CFCC ranged from 2.39 to 2.63 g/cm^3, and the porosity volume percentage of the composite disk was about 15%. The flexural test bars were machined by a diamond saw with actual final dimensions, about 0.4 cm long, 0.3 cm wide and 0.2–0.25 cm thick. The flexural strength was obtained by the four-point bending technique [1–3,6].

3. The establishment of the computation model

3.1. The classical laminated plate theory [9–13]

The classical laminated plate theory gives the most useful guidelines for estimating the stress–strain relationship for the laminated structures. According to the theory, the stresses, $[\sigma]_{x,y}$, can be obtained by multiplying the strains $[\varepsilon]_{x,y}$ with the reduced stiffness matrix after the transformation to the x–y coordinate system, $[\bar{Q}]_{x,y}$, i.e.,

$$[\sigma]_{x,y} = [\bar{Q}][\varepsilon]_{x,y}. \tag{1}$$

$[\bar{Q}]$ can be estimated from the relation

$$[\bar{Q}] = [T]^{-1}[Q][T]^{\mathrm{T}}, \tag{2}$$

where $[Q]$ is the reduced stiffness matrix with fibers in the lamina parallel to one of the x and y axes, $[T]^{-1}$ is the inverse matrix of $[T]$, $[T]^{\mathrm{T}}$ is the transpose matrix of $[T]$. $[T]$ is the force transformation matrix when the lamina is rotated at a certain angle, θ, which is expressed by

$$[T] = \begin{bmatrix} \cos^2\theta & \sin^2\theta & 2\sin\theta\cos\theta \\ \sin^2\theta & \cos^2\theta & -2\sin\theta\cos\theta \\ -\sin\theta\cos\theta & \sin\theta\cos\theta & \cos^2\theta - \sin^2\theta \end{bmatrix}. \tag{3}$$

When $[\bar{Q}]_{x,y}$, the reduced stiffness matrix after the transformation to the x–y–z coordinate system, of a certain layer is calculated, the relations among the resultant loading force, N, and moment, M, and reference plane strains, $[\varepsilon_0]$, and laminate curvatures, $[k]$, can be obtained by the equation

$$\begin{bmatrix} N \\ M \end{bmatrix} = \begin{bmatrix} A & B \\ B & D \end{bmatrix} \begin{bmatrix} \varepsilon^0 \\ k \end{bmatrix}, \tag{4}$$

where A is the extensional stiffnesses, B, the coupling stiffnesses, and D, the flexural laminate stiffnesses, which can be related to the $[\bar{Q}]_{x,y}$ by the formula

$$(A_{ij}, B_{ij}, D_{ij}) = \sum_{L=1}^{n} \int_{H_{L-1}}^{H_L} (1, z, z^2)\bar{Q}_{ij}\,\mathrm{d}z, \tag{5}$$

where z is the coordinate variable in the z-axis (the laminate thickness direction), H_L, H_{L-1} are the z-coordinates of the upper and lower surfaces of the Lth lamina.

If Eq. (4) is rewritten by performing matrix inversions, it becomes

$$\begin{bmatrix} \varepsilon^0 \\ k \end{bmatrix} = \begin{bmatrix} a & b \\ b & d \end{bmatrix} \begin{bmatrix} N \\ M \end{bmatrix}, \tag{6}$$

where matrices, $[a]$, $[b]$ and $[d]$, are the laminate compliance matrices which can be obtained from the stiffness matrices as follows:

$$\begin{aligned} [a] &= [A^{*-1}] - \{[B^*][D^{*-1}]\}[C^*], \\ [b] &= [B^*][D^{*-1}], \\ [c] &= -[D^{*-1}][C^*], \\ [\mathrm{d}] &= [D^{*-1}] \end{aligned} \tag{7}$$

and

$$\begin{aligned} [A^{-1}] &= \text{inverse of matrix } [A], \\ [B^*] &= -[A^{-1}][B], \\ [C^*] &= [B][A^{-1}], \\ [D^*] &= [D] - \{[B][A^{-1}]\}[B]. \end{aligned}$$

3.2. The computation of the effective elastic moduli

We assume that the composite test bars, machined from a similar location in the same disk, have similar fiber strengths (with a similar Weibull distribution of strength and a similar extent of fiber strength degradation) and FCVI infiltration results, i.e., similar coating adhesion and interfacial coating thickness as well as a similar porosity distribution. In other words, except for the lamina stacking sequence, all other factors of the lamina that form the laminate are, statistically, the same. In this way, the CFCCs can be treated, macroscopically, as a laminate stacked with laminae (plain-weave fibber fabrics) that have, statistically, the same properties. Thus, a relationship between the lamina stacking sequence and laminate effective mechanical properties can be obtained by the classical laminated plate theory [9–13].

For simplicity, the derivation of the expression for the effective elastic moduli can be started from a symmetric case. For the symmetric laminates, Eq. (6) reduces to

$$\begin{bmatrix} \varepsilon_x^0 \\ \varepsilon_y^0 \\ \gamma_s^0 \end{bmatrix} = \begin{bmatrix} a_{xx} & a_{xy} & a_{xs} \\ a_{yx} & a_{yy} & a_{ys} \\ a_{sx} & a_{sy} & a_{ss} \end{bmatrix} \begin{bmatrix} N_x \\ N_y \\ N_s \end{bmatrix}, \tag{8}$$

where $[a]$ is the extensional laminate compliance matrix, which is $[a] = [A]^{-1}$, and ε_x^0, ε_y^0 and γ_s^0 are the in-plane and shear strain components in the reference plane.

If we treat the symmetric laminate as a homogeneous orthotropic material on a macroscopic scale, its elastic behavior will be similar to that of a unidirectional lamina. Thus, the concept of average stresses and strains and effective laminate constants can be employed. Given the total thickness, tt, of the laminate, then, the average stresses, $[\bar{\sigma}]$, can be related to the loading $[N]$, i.e.,

$$\begin{bmatrix} \bar{\sigma}_x \\ \bar{\sigma}_y \\ \tau_s \end{bmatrix} = \begin{bmatrix} N_x \\ N_y \\ N_s \end{bmatrix} \frac{1}{\mathrm{tt}}, \tag{9}$$

where $\bar{\sigma}_x$, $\bar{\sigma}_y$ and $\bar{\gamma}_s$ are the average in-plane and shear stress components of $[\bar{\sigma}]$. The strain–force relation for the laminate in terms of engineering constants is

$$\begin{bmatrix} \varepsilon_x^0 \\ \varepsilon_y^0 \\ \gamma_s^0 \end{bmatrix} = \begin{bmatrix} 1/\bar{E}_{xx} & -\bar{\nu}_{yx}/\bar{E}_y & \bar{\eta}_{sx}/\bar{G}_{xy} \\ -\bar{\nu}_{xy}/\bar{E}_x & 1/\bar{E}_y & \bar{\eta}_{sy}/\bar{G}_{xy} \\ \bar{\eta}_{xs}/\bar{E}_x & \bar{\eta}_{ys}/\bar{E}_y & 1/\bar{G}_{xy} \end{bmatrix} \begin{bmatrix} N_x \\ N_y \\ N_s \end{bmatrix} \frac{1}{\mathrm{tt}}, \tag{10}$$

where $\bar{E}_x$ and $\bar{E}_y$ are the laminate effective Young's moduli in the x- and y-directions; $\bar{\nu}_{xy}$ and $\bar{\nu}_{yx}$ are the laminate effective Poisson's ratios, and $\bar{\eta}_{xs}$, $\bar{\eta}_{ys}$, $\bar{\eta}_{sx}$ and $\bar{\eta}_{sy}$ are laminate effective shear coupling coefficients.

By equating the corresponding terms in the compliance matrices of Eqs. (8) and (10), the expressions for the laminate effective moduli can be obtained as

$$\bar{E}_x = \frac{1}{\mathrm{tt} * a_{xx}}, \qquad \bar{E}_y = \frac{1}{\mathrm{tt} * a_{yy}}, \qquad \bar{G}_{xy} = \frac{1}{\mathrm{tt} * a_{ss}}. \tag{11}$$

Although Eq. (11) was derived from a symmetric laminate, since the a_{xx}, a_{yy} and a_{ss} in Eq. (11) were obtained from Eq. (7), i.e., the contribution of both the resultant loading, N, and the resultant moment, M, has already been taken into account. As a result, Eq. (11) is also valid for a more generalized case, such as non-symmetric laminates.

3.3. The computation of the effective stiffness matrix [Q] for a lamina with plain-weave reinforcements

As the CFCC under study is composed of multiple plies of plain-weave (2D, 0°/90°) laminae, the calculation of $[Q]$, the reduced stiffness matrix in the x–y–z coordinate system, becomes more complex. One of the models that can best reveal the plain-weave geometry is the fiber undulation model developed by Ishikawa and Chou [14]. The undulation model depicting the woven structure geometry can be expressed by the following geometrical parameters, $h_1(x)$, $h_2(x)$ and a_u, which are functions of the x coordinate, as is shown in Fig. 2 [14]:

$$h_1(x) = \begin{cases} 0 & (0 \le x \le a_0) \\ [1+\sin\{(x-\frac{1}{2}a)\pi/a_u\}]h_t/4 & (a_0 \le x \le a_2) \\ \frac{1}{2}h_t & (a_2 \le x \le n_g a/2) \end{cases} \tag{12}$$

$$h_2(x) = \begin{cases} 0 & (0 \le x \le a_0) \\ [1-\sin\{(x-\frac{1}{2}a)\pi/a_u\}]h_t/4 & (a_0 \le x \le a/2) \\ -[1+\sin\{(x-a/2)\pi/a_u\}]h_t/4 & (a/2 \le x \le a_2) \\ -\frac{1}{2}h_t & (a_2 \le x \le n_g a/2) \end{cases} \tag{13}$$

where n_g is a basic geometrical parameter to characterize a fabric, which equals to 2 for a plain-weave structure, h_t is thickness of the fiber layer. The parameters

$$a_0 = (a - a_u)/2 \tag{14}$$

$$a_2 = (a + a_u)/2 \tag{15}$$

can be determined by specifying a_u, which is geometrically arbitrary in the range from 0 to a.

Now, all the components in Eqs. (5) and (6), i.e., Q, A, B, and D matrices, become the functions of the undulation structure-governing factor, the distance x, i.e., $Q(x)$, $A(x)$, $B(x)$, $D(x)$. Putting these matrix functions back into Eqs.

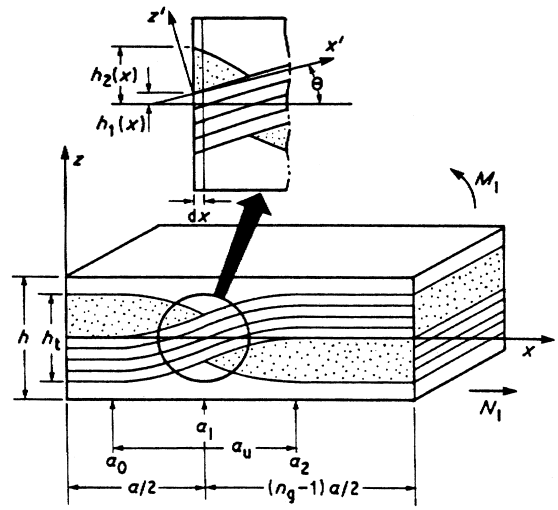

Fig. 2. Illustration for the fiber undulation model (after Ishikawa and Chou [14]).

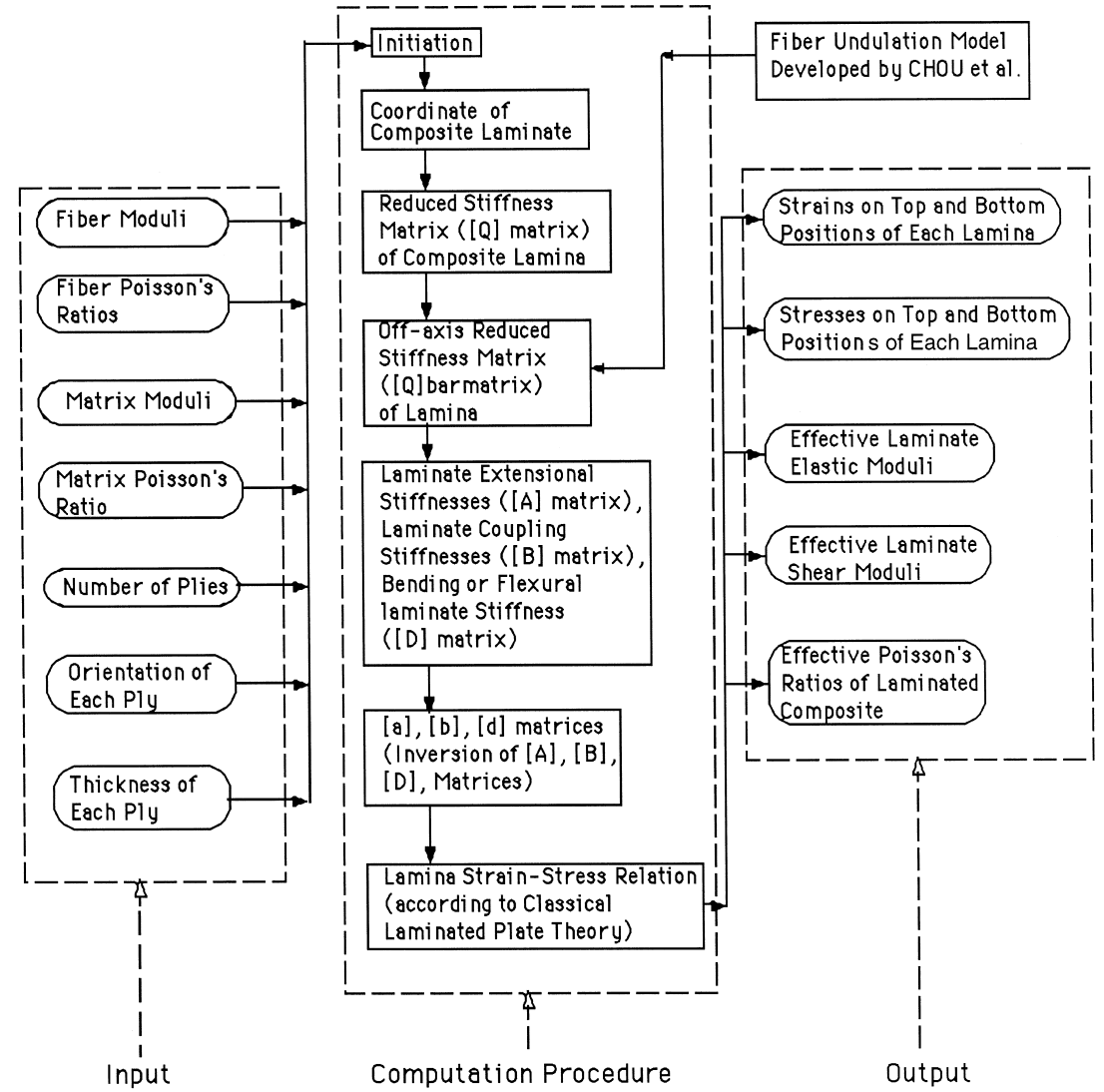

Fig. 3. Flowchart for the computation procedures of the Fortran program.

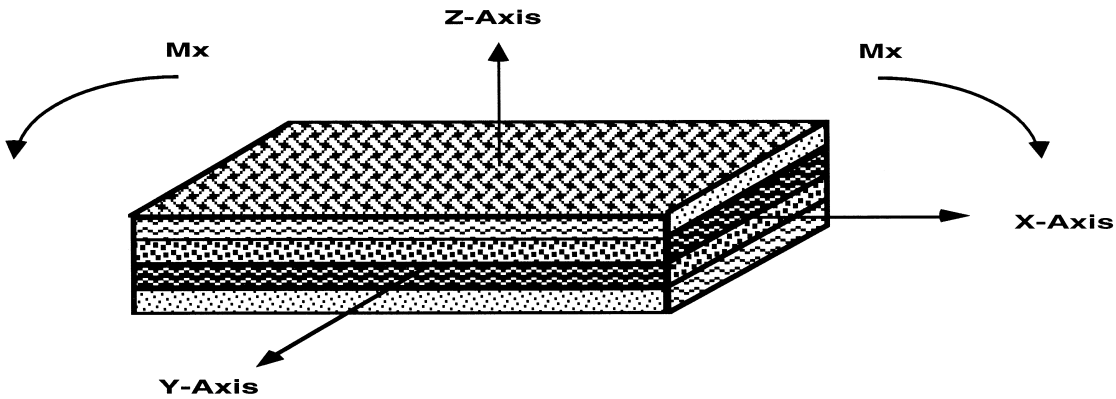

Fig. 4. Schematic diagram for the coordinate system of flexural testing.

Table 1
Six possible stacking sequences of the lay-up $[0/30/60]_4$

Ply no.	$[0/30/60]_4$	$[60/30/0]_4$	$[30/60/0]_4$	$[0/60/30]_4$	$[60/0/30]_4$	$[30/0/60]_4$
12th	60	0	0	30	30	60
11th	30	30	60	60	0	0
10th	0	60	30	0	60	30
9th	60	0	0	30	30	60
8th	30	30	60	60	0	0
7th	0	60	30	0	60	30
6th	60	0	0	30	30	60
5th	30	30	60	60	0	0
4th	0	60	30	0	60	30
3rd	60	0	0	30	30	60
2nd	30	30	60	60	0	0
1st	0	60	30	0	60	30

(4)–(6), we developed a Fortran program for the computation of the in-plane elastic stress distribution in the laminate, Fig. 3.

3.4. Computer modeling procedures

A Fortran program was written for a SUN workstation to quantify the stacking sequence effect on the effective elastic moduli of the plain-weave fiber fabric-reinforced laminated composite. As discussed before, the theoretical model was established, principally, based on the classical laminate plate theory [9–13]. The effective reduced stiffness matrix of the woven geometry was calculated using a fiber undulation model developed by Ishikawa and Chou [14]. The establishment of the computation model is described as follows [15,16]. Fig. 3 shows the flowchart for computation procedures of the Fortran program we developed. In the input file, one needs to provide the elastic moduli and Poisson's ratios of the fiber and matrix materials, the number of plies, the thickness of each lamina, the fiber orientation in the fiber fabric plane of each lamina, and the load and/or moment applied. From the output, one can obtain the values of the laminate effective elastic moduli. Fig. 4 is the coordinate system for the computation, the x, y and z axes are the longitudinal, the transverse, and the thickness directions of the bend bar, respectively, and the tensile surface is on the upper side of the bend bar.

Table 2
Stacking sequences for laminates with 10 to 13 plies

Number	10-layer	11-layer	12-layer	13-layer
13th				0
12th			60	60
11th		30	30	30
10th	0	0	0	0
9th	60	60	60	60
8th	30	30	30	30
7th	0	0	0	0
6th	60	60	60	60
5th	30	30	30	30
4th	0	0	0	0
3rd	60	60	60	60
2nd	30	30	30	30
1st	0	0	0	0

3.5. The input data

The thickness of the flexural test bar is usually 0.3 cm. The average thickness of the Nicalon woven cloth is 0.0254 cm. Thus, the 0.3 cm thick test bar contains roughly 12 layers. Because the fill and the warp threads in the plain-weave fabric are of the same fiber materials, the mechanical properties of the fabric are the same for orthotropic (right angle) directions, i.e., the mechanical properties of the fabric in the 0° direction is the same as that in the directions of 90°, 180° and 270°. Therefore, it is the same case with directions of 30°, 120°, 210° 300° and 60°, 150°, 240° 330°, for the $[0/30/60]$ lay-up. Since the orientation of adjacent layers can be rotated 30° clockwise or counterclockwise, altogether, there are only six stacking sequences within the $[0/30/60]$ lay-up family, i.e., $[0/30/60]_4$, $[60/30/0]_4$, $[30/60/0]_4$, $[0/60/30]_4$, $[60/0/30]_4$ and $[30/0/60]_4$, as shown in Table 1. Some of the specimens are ~ 0.25 cm thick. This indicates that the number of laminae that form these specimens is not the same. If the thickness of these specimens ranges from 0.25

Table 3
Elastic properties of Nicalon fiber and FCVI-SiC matrix

Items	Elastic modulus (GPa)	Shear modulus (GPa)	Poisson's ratio
Nicalon fiber	190	85	0.12
FCVI-SiC matrix	400	154	0.30

cm to 0.32 cm, these laminates contain 10 to 13 plies. Their possible stacking sequences are listed in Table 2. Table 3 lists the material properties of the Nicalon fiber and the FCVI-SiC matrix. A loading moment of 500 Pa m^3 is assumed to be applied to the laminate for numerical calculations.

4. Results and discussion

4.1. The effect of the lamina stacking sequence on effective elastic moduli of the laminated composite.

Fig. 5 presents the relationship between the effective elastic moduli of the laminated composite and the stacking sequence for the [0/30/60] lay-up. As expected, a different stacking sequence contributes to the variation of effective elastic moduli.

4.1.1. The effect of different stacking sequence with a fixed ply number

The results show that different stacking sequences within the same lay-up of a composite with a fixed ply number will give various effective elastic moduli of the laminated composites. For example, for a laminate with 11 plies, if the laminate is stacked up by the sequence of repeating the stacking series of [0/30/60], the effective elastic modulus in *x*-axis is 253.8 GPa; if the laminate is stacked up by the sequence of repeating the stacking series of [30/60/0], the effective elastic modulus in *x*-axis is 233.9 GPa; if the laminate is stacked up by the sequence of repeating the stacking series of [60/0/30], the effective elastic modulus in *x*-axis is 238.5 GPa. So it is with the effective elastic modulus in the *y*-axis. The same trend is also observed for the ply number of 10 and 13. Thus, if the laminates have different stacking sequences, the magnitude of the effective elastic modulus will be different, even if the laminates are of the same materials and under the same loading condition (Table 1 and Fig. 5). However, one important feature in Fig. 5 is that 12 is a good number of plies for the [0/30/60] lay-up, since with this number of plies, the effective elastic modulus is not sensitive to the stacking sequence for the [0/30/60] lay-up. The reason is probably that 12 is an integer multiplier of the number of possible lamina fiber orientations, i.e., 3, in the [0/30/60] lay-up. This indicates that it is possible to minimize the stacking sequence effect on elastic moduli, if we choose the right number of plies for a given lay-up.

4.1.2. The effect of ply number

A difference in the effective elastic modulus may also occur for laminates containing different numbers of plies. Although the two laminates have the same type of lay-up, and are arranged by the same repetition of the lamina, the difference in the number of plies gives the variation in the exact stacking sequences of the two laminates (Table 2 and Fig. 5). For the same stacking series, say [0/30/60], if the laminate has 10 plies, the effective elastic modulus in *x*-axis is 262.5 GPa; if the laminate has 11 plies, the effective elastic modulus in *x*-axis is 253.8 GPa; if the laminate has 12 plies, the effective elastic modulus in *x*-axis is 248.6 GPa; if the laminate has 13 plies, the effective elastic modulus in *x*-axis is 258.8 GPa. It is obviously seen that the effective elastic modulus varies with the different number of plies, and the [0/30/60] stacking series usually gives a higher magnitude, but follows no steady rules. This trend reveals that the thickness of the specimen affects the effective elastic modulus of the composite. This suggests that there is a difference in the effective elastic modulus, and thus, it is difficult to com-

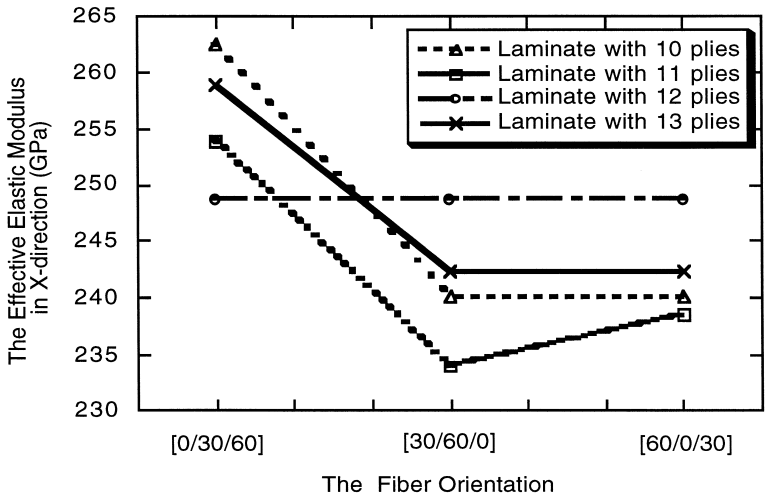

Fig. 5. Calculated stacking sequence effect on the effective elastic moduli of laminated CFCCs (lay-up [0/30/60]), under an assumed bending moment of 500 Pa m^3.

pare strength values obtained from CFCC specimens with different thicknesses.

4.2. The effect of lamina stacking sequence on flexural strength of the laminated composite through varying the laminate effective moduli

Beside the effects on the variation of laminate effective elastic moduli, shown in Fig. 5, our previous results revealed that the lamina stacking sequence can also affect the matrix-cracking stress of a laminated composite, Figs. 6 and 7 [15,16]. The latter leads to the variation in the internal stress distribution of the laminate, which indicates that laminates with different stacking sequences can, probably, bear different external loads. Furthermore, because the maximum stresses are located at different plies in two composites with different stacking sequences, this trend will probably lead to crack initiation at difference sites in the laminate thickness direction. This behavior will also contribute to difference in composite failure modes. Eventually, these results will cause a variation in the extent of energy-dissipating toughening mechanisms of CFCCs, such as fiber pullout and bridging.

The stress–strain curve of a CFCC is composed of two portions. One is the linear elastic region, where the end point represents the matrix-cracking stress, and the slope of the line stands for the effective elastic moduli of the CFCC laminate. The other is the non-linear portion of the curve that represents the load transferring from the matrix to fiber after the matrix crack initiation until the eventual fiber pullout. The shape of this portion of the curve is mainly dependent on the composite system, the percentage of the reinforcement, the fiber strength, and the fiber/matrix interfacial behavior, as mentioned before. The implication is that difference in the stress–strain curves of CFCCs may be simply caused by the variation in the end points of the linear part, which is also the starting point of the nonlinear part, and the difference in the shape of the nonlinear part. For the CFCCs in the present study, we can roughly construct the flexural stress–strain curve from two cases; one assumes that the nonlinear portion maintains approximately the same shape, and the other considers variations in the shape of the nonlinear portion, as discussed below.

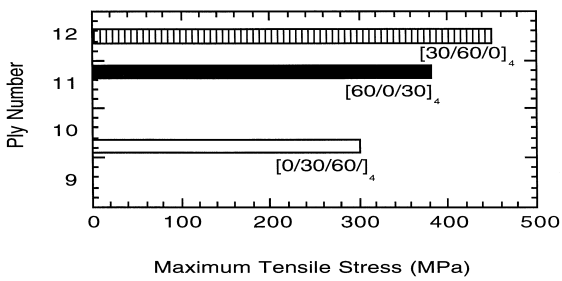

Fig. 6. Calculated maximum tensile stresses for different stacking sequences of the [0/30/60] lay-up, under an assumed bending moment of 500 Pa m^3.

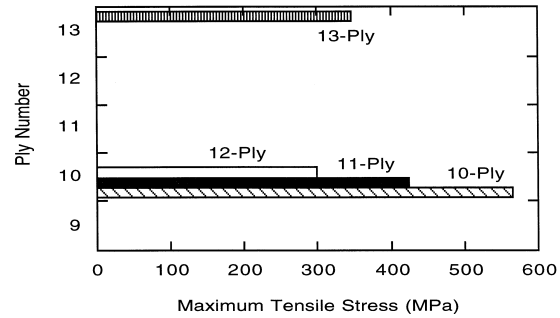

Fig. 7. Calculated maximum tensile stresses for different stacking sequences of the [0/30/60] stacking series, under an assumed bending moment of 500 Pa m^3.

4.2.1. Case 1: The similarly shaped nonlinear portion

The specimens in the present study have the same matrix/fiber system, the same fiber volume percentage, and the same type of interfacial coatings. If they are taken from the same depth positions in the disk, i.e., minimizing the factor regarding the difference in the fiber strength degradation due to the high-temperature damage during FCVI processing, all other mechanical properties are the same except for the difference in the stacking sequence. In this case, just for simplicity and for the first order of estimation, we can assume that the shape of the non-linear portion of the CFCC stress–strain curve always remains the same for a given interface. This means that differences in the predicted stress–strain curves may be viewed as variation in the end points of the linear portion, which is also the starting point of the nonlinear portion. If the laminates with different stacking sequences have the same moduli, e.g., for the laminate with 12 plies, the contribution to the difference of laminate internal stress distributions can be schematically shown in Fig. 8(a). The difference in the matrix-cracking stress leads to different starting points of the non-linear portion, which can give a different peak stress on the curve, i.e. the different ultimate strengths of the CFCC. In other words, the stacking sequence of $[0/30/60]_4$ gives the highest level of the stress–strain curve, while the $[30/60/0]_4$ yields the lowest level among the stacking sequences of $[0/30/60]_4$, $[30/60/0]_4$ and $[60/0/30]_4$, Fig. 8(a). This trend could result from the fact that the $[0/30/60]_4$ has the lowest maximum tensile stress, Fig. 6, i.e., it has the highest matrix-cracking stress, while the $[30/60/0]_4$ has the highest maximum tensile stress and the lowest matrix-cracking stress [15,16]. Fig. 8(b) illustrates the case when the stacking sequences lead to variations in both the matrix-cracking stress and the laminate effective elastic moduli. Both the end point and the slope of the linear portion of the stress–strain curve

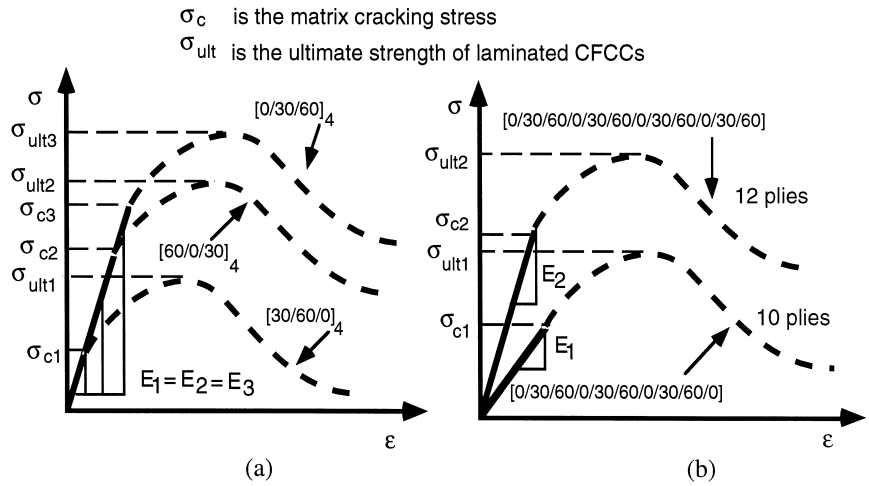

Fig. 8. Illustrations of the contributions of stacking sequence effect on the flexural strength of CFCCs by varying the matrix cracking stress and laminate effective elastic modulus: (a) three stacking sequences having the same effective moduli, but different matrix cracking stresses; (b) two stacking sequences having different stacking series and different laminate effective elastic moduli.

can contribute to differences in the final peak stress of the whole stress–strain curves.

4.2.2. Case 2: Differently shaped nonlinear portion

As previously mentioned, differences in the locations of the matrix-cracking stress may lead to variations in the laminate failure modes, which may contribute to different extents of the energy-dissipating toughening mechanisms. These will change the shape of the nonlinear portion of the stress–strain curve of the CFCCs. In this case, the difference in both the starting point and the shape of the non-linear portion will lead to a different peak stress on the stress–strain curve, i.e., a scatter in the flexural strength of the CFCC.

The stacking sequence effect can be a reason for the scatter observed in the flexural strengths of CFCCs. The effect influences the flexural strength of laminate by changing the internal stress distribution within the laminate. This trend can lead to variations in the three aspects of the laminate: (i) the matrix-cracking stress, which yields a different starting point of the nonlinear portion of the flexural stress–strain curve; (ii) the effective laminate elastic moduli, which give the different slopes to the linear portion of the flexural stress–strain curve and that also changes the position of the starting point of the non-linear portion; (iii) the laminate failure modes, which may lead to different extents of the energy-dissipating mechanisms and that will change the shape of the non-linear portion. Differences in the starting point and the shape of the non-linear portion will lead to different peak stresses in the stress–strain curves, i.e., a scatter in the flexural strengths of the CFCCs. The effect will be more evident, if the specimens have varying thicknesses, and if the fiber, matrix, interfacial coating thickness and porosity are more evenly distributed. Although the [0/30/60] lay-up is quasi-isotropic, after being cut into flexural samples, the composite bend bars become laminates with non-identical stacking sequences, due to the difficulty in machining. Variations in the laminate stacking sequences can override the initial design purpose, the quasi-isotropic nature of the [0/30/60] lay-up. The characteristics of the mechanical performance of the CFCCs with the [0/30/60] lay-up can be more accurately understood using the flexural strength, if the stacking sequence effect of the CFCCs can be taken into account.

5. Conclusions

The effective elastic moduli of a plain-weave Nicalon fiber-fabric reinforced SiC-matrix ceramic composites with a [0/30/60] lay-up were computed. Lamina stacking sequence, including variations in stacking series and ply numbers, can lead to differences in the effective elastic moduli of a laminated CFCC. The trend, combined with its effects on the in-plane elastic stress distributions, may contribute to the scattering of flexural strengths of CFCC.

Acknowledgements

The research is sponsored by the National Science Foundation project on ceramic-matrix composites (CMCs) under contract no. NSF EEC-9527527 to The University of Tennessee at Knoxville (UTK), with Mrs M. Poats as the program monitor. Thanks also go to Dr W.A. Curtin of Virginia Polytechnic Institute and State University, and Dr C.-H Hseuh, Dr T.M. Besmann, Dr D.P. Stinton and Dr

E.R. Kupp of the Oak Ridge National Laboratory for their encouragement, valuable suggestions, and discussions.

References

[1] D.P. Stinton, A.J. Caputo, R.A. Lowden, Ceram. Bull. 65 (2) (1986) 347.
[2] D.P. Stinton, T.M. Besmann, R.A. Lowden, Ceram. Bull. 67 (2) (1988) 350.
[3] T.M. Besmann, B.W. Sheldon, R.A. Lowden, D.P. Stinton, Science 253 (1991) 1104.
[4] P.K. Liaw, D. K Hsu, N. Yu, N. Miliyala, V. Saini, H. Jeong, Acta Mater. 44 (5) (1996) 2101.
[5] P.K. Liaw, N. Yu, D.K. Hsu, N. Miriyala, V. Saini, L.L. Snead, C.J. McHargue, R.A. Lowden, J. Nucl. Mater. 219 (1995) 93.
[6] J.H. Miller, R.A. Lowden, P.K. Liaw, in: Symp. on Ceramic Matrix Composite — Advanced High-Temperature Structural Materials, R.A. Lowden et al. (Eds.), Materials Research Society, vol. 365, 1995, p. 403.
[7] K.R. Vaidyanathan, J. Sankar, A.D. Kelkar, J. Narayan, Ceram. Eng. Sci. Proc., July–Aug., 1994, pp. 281–291.
[8] W.S. Steffier, Ceram. Eng. Sci. Proc., Sept.–Oct., 1993, pp. 1045–1057.
[9] R.M. Christensen, Mechanics of Composite Materials, Wiley, New York, 1979.
[10] I.M. Daniel, O. Ishai, Engineering Mechanics of Composite Materials, Oxford University, 1994.
[11] R.M. Jones, Mechanics of Composite Materials, Scripta, 1975.
[12] D. Hull, An Introduction to Composite Materials, Cambridge University, 1981.
[13] J.C. Halpin, Primer on Composite Materials: Analysis, Technomic, 1984.
[14] T. Ishikawa, T.-W. Chou, J. Mater. Sci. 17 (1982) 3211.
[15] W. Zhao, P.K. Liaw, N. Yu, Ceram. Sci. Eng. Proc., 1997, pp. 401–408.
[16] W. Zhao, P.K. Liaw, N. Yu, The reliability of evaluating the mechanical performance of continuous fiber-reinforced ceramic composites by flexural testing, Proc. 1st Int. Conf. on Maintenance and Reliability, Knoxville, Tennessee, May 1997, pp. 1-15.